Original article

Inhibition of biofilm formation by alpha-mangostin loaded nanoparticles against *Staphylococcus aureus*

Phuong T.M. Nguyen [a,b,*], Minh T.H. Nguyen [c], Albert Bolhuis [d,*]

[a] *Institute of Biotechnology, Vietnam Academy of Science and Technology, 18 Hoang Quoc Viet Road, Cau Giay, Hanoi, Viet Nam*
[b] *Graduate University of Science and Technology, Vietnam Academy of Science and Technology, 18 Hoang Quoc Viet Road, Cau Giay, Hanoi, Viet Nam*
[c] *University of Science and Technology of Hanoi, Vietnam Academy of Science and Technology, 18-Hoang Quoc Viet Road, Cau Giay, Hanoi, Viet Nam*
[d] *Department of Pharmacy and Pharmacology, University of Bath, Claverton Down, Bath BA2 7AY, UK*

A B S T R A C T

This study aimed to investigate the antibiofilm activity of alpha-mangostin (AMG) loaded nanoparticles (nanoAMG) against *Staphylococcus aureus*, including the methicillin-resistant strain MRSA252. The results indicated that treatment with 24 μmol/L nanoAMG inhibited the formation of biofilm biomass by 53–62%, compared to 40–44% for free AMG ($p < 0.05$). At 48 μmol/L, biofilms in all nanoAMG treated samples were nearly fully disrupted for the two tested strains, MRSA252 and the methicillin-sensitive strain NCTC6571. That concentration resulted in killing of biofilm cells. A lower concentration of 12 μmol/L nanoAMG inhibited initial adherence of the two bacterial strains by > 50%. In contrast, activity of nanoAMG was limited on preformed mature biofilms, which at a concentration of 48 μmol/L were reduced only by 27% and 22% for NCTC6571 and MRSA252, respectively. The effects of AMG or nanoAMG on the expression of biofilm-related genes showed some noticeable differences between the two strains. For instance, the expression level of *ebpS* was downregulated in MRSA252 and upregulated in NCTC6571 when those strains were treated with either AMG or nanoAMG. In contrast, the expression of *fnbB* was down regulated in NCTC6571, while it was up-regulated in the MRSA252. The expression of other biofilm-related genes (*icaC*, *clfB* and *fnbA*) was down regulated in both strains. In conclusion, our results suggest that AMG coated nanoparticles had enhanced biological activity as compared to free AMG, indicating that nanoAMG could be a new and promising inhibitor of biofilm formation to tackle *S. aureus*, including strains that are resistant to multiple antibiotics.

© 2020 The Authors. Published by Elsevier B.V. on behalf of King Saud University. This is an open access article under the CC BY-NC-ND license (http://creativecommons.org/licenses/by-nc-nd/4.0/).

1. Introduction

Biofilm-related bacterial infections cause significant problems, as bacteria in biofilms are more tolerant to antibiotics (Fey, 2010; Flemming and Wingender, 2009; Hall-Stoodley and Stoodley, 2009; Dastgheyb et al., 2014). Biofilm-producing bacteria account for about two-thirds of human bacterial infections. There-fore, novel strategies for battling clinically relevant biofilms are urgently needed.

Staphylococcus aureus (SA) biofilms are associated with chronic infections and contaminated medical devices, such as in native valve endocarditis, bone tissue infections, and chronically infected wounds. The presence of a biofilm renders the bacteria highly tolerant to antibiotics and capable of resisting phagocytosis (Kong et al., 2018; Archer et al., 2011). SA strains usually have either a polysaccharide intercellular adhesion (PIA)-associated biofilm or a protein-mediated biofilm, which depends on the strain and environmental conditions (Foulston et al., 2014; Phitaktim et al., 2016; Vergara-Irigaray et al., 2009; Oniciuc, et al., 2016; O'Neill et al., 2008; Burke et al., 2010; Speziale et al., 2014; Shivaee et al., 2019). Interestingly, protein-mediated biofilms seem to be formed frequently by highly virulent MRSA isolates, demonstrating a special role of this biofilm structure (O'Neill et al., 2008; Greenberg et al., 2008).

α-Mangostin (AMG) is a natural xanthone from mangosteen (*Garcinia mangostana* L) grown in Vietnam, and the pericarp is particularly rich in this compound. It has been reported to have valuable bioactive properties which includes antimicrobial, antiinflamatory, anticancer, antifungal, antiviral, and antioxidant activities (Ibrahim et al., 2016; Wang et al., 2017). It is, for instance, an effective antimicrobial agent against biofilm-forming *Streptococcus mutans*, a cariogenic organism, through disruption of the development, acidogenicity, and/or the mechanical stability of *S. mutans* biofilms (Nguyen et al., 2014). Recently, it was found to inhibit biofilm production by *Staphylococcus epidermidis, Acinetobacter baumannii* and *S. aureus* biofilms, including MRSA strains (Nguyen et al., 2017; Sivaranjani et al., 2017; Sivaranjani et al., 2018). However, the potential use of AMG to prevent biofilm formation for clinical purposes is complicated due to its low water solubility. To improve its biological activity, we have prepared AMG loaded nanoparticles (nanoAMG) to enhance the availability of AMG and consequently to enhance its antibiofilm activity for application purposes (Gunasekaran et al., 2014; Koo et al., 2017; Rabin et al., 2015). AMG was tested *in vitro* for anti-biofilm activity using *S. aureus* strains MRSA252 (which forms protein-based biofilms) and NCTC6571 (polysaccharide-based biofilm) (Nguyen et al., 2017). We report for the first time the effects of synthesized nanoAMG on *S. aureus* adherence, biofilm formation and eradication, and the expression of genes involved in those processes.

2. Materials and methods

2.1. Bacteria and growth conditions

S. aureus (SA) strains, which included the standard strain NCTC6571 and the clinical isolate MRSA 252 (Holden et al., 2004), were aerobically cultured in tryptic soy broth (TSB) medium (Difco) at 37 °C. For biofilm growth, the medium was supplemented with 0.5% glucose (TSBg).

2.2. Isolation of AMG

AMG from *G. mangostana* peels was prepared as described elsewhere (Nguyen et al., 2017). The obtained AMG with a purity level exceeding 98% (HPLC) was identified by ^{1}H and ^{13}C – nuclear magnetic resonance (NMR).

2.3. Preparation of nanoAMG

AMG loaded polymeric nanoparticles were prepared using Tween 20 (Sigma) and PEG 400 (Sigma) based on a method described by Nguyen et al. (2020) NanoAMG was characterized using a dynamic light scattering machine (DLS - HORIBA SZ-100 analyzer, Germany). The nanoparticle sizes were in a range of 10–50 nm with a zeta potential value of − 35.20 mV and a polydispersity index (PI) was < 0.3 (Fig. A). The infrared spectrum data (Fig. B) showed the incorporation of AMG in the carriers (Nguyen et al., 2020).

2.4. Biofilm assay in 96-well microtiter plate

S. aureus was cultured overnight in TSBg and diluted for biofilm growth in 96-well polystyrene plates. To measure the effect of biofilm formation, different concentrations of AMG (stocks prepared in ethanol) or nanoAMG (prepared in water) were also added to the wells. The plates were then incubated at 37 °C on a 3-dimensional rocking plate. After 24 h of growth the medium was replaced with fresh medium containing the same concentration of AMG or nanoAMG, and the plates were incubated for a further 24 h. Planktonic cells were then removed and the biofilms were washed 3 times with sterile PBS. Next, the plates were dried for 1 h at 60 °C, and biofilms were stained with crystal violet solution (0.1% w/v) for 15 min. The crystal violet was then removed and the plates were washed gently with water. The absorbed crystal violet was dissolved in 30% v/v acetic acid and the absorbance was quantified at λ = 595 nm (A_{595}) (Alhusein et al., 2013). To measure the effect of biofilm eradication, cells were first grown in the absence of AMG or nanoAMG for 24 h, and then the medium was replaced with fresh medium containing different concentrations of AMG or nanoAMG. The plates were incubated for a further 24 h, and the biofilms were then washed, stained, and quantified as above.

2.5. Bacterial adhesion assay

The quantification of bacterial adhesion was performed by using the crystal violet staining technique according to Rodrigues et al., (2006). The adhesion tests were performed by dispensing 200 μL of bacterial suspensions, prepared as previously described, in a 96 well polystyrene microtiter plate. The time of contact for the adhesion of cells to polystyrene was 4 h. Unattached cells were removed by washing the wells three times with water, and the adherent microorganisms were fixed with 200 μL of methanol for 15 min. The wells were then stained for 15 min with 200 μL crystal violet (1% w/v aqueous solution), rinsed under the running tap water and left to dry. The bound dye was resuspended with 200 μL of glacial acetic acid (33% v/v) and the absorbance of each well was measured using an automated plate reader (Thermoplate) at 630 nm.

2.6. Confocal microscopy

Polyvinyl plastic coverslips (22 mm × 22 mm) were sterilized in absolute isopropanol and then dried and placed in a 6-well culture plate. An aliquot (2 mL) of a diluted bacterial suspension in TSBg was added. To test inhibition of the formation of biofilms, AMG was added to the wells at the start of biofilm growth. To test disruption and/or killing of preformed biofilms, biofilms were grown for 24 h, followed by removal of planktonic cells and addition of fresh medium containing nanoAMG. The 6-well plate was incubated at 37 °C for a further 24 h, then the culture medium was removed and the coverslips were washed 3 times with sterile water. To assess the effectiveness of the agents, biofilms were stained with 0.3% v/v LIVE/DEAD BacLight mixture of dye solution in sterile water. The coverslips were left for 15 min in the dark prior to washing again with sterile water. Then the coverslips were mounted on glass slides and sealed with nail varnish. Stained biofilms were observed using laser scanning confocal fluorescence microscopy (Olympus, Tokyo, Japan). The image data were processed with Imaris software (Bitplane AG, Zürich, Switzerland).

2.7. Reverse transcription quantitative PCR (qRT-PCR)

qRT-PCR was performed to evaluate the expression of the selected *fnbA, fnbB, ebpS, icaC, clfB* genes that are related to biofilm adhesion and synthesis by *S. aureus*. These genes were found to have the biggest changes in expression level compared to other genes during biofilm formation by SA (Atshan et al., 2013). The time point of 24 h biofilm growth was chosen for treatment based on data reported by Atshan et al. (2013). In this experiment, biofilms were grown in 24 well plastic plates (Costar, USA) in presence of the test agents at 12 μmol/L for 24 h. After treatment, biofilms were washed twice with 0.9% NaCl. The adhering bacterial cells in each well were disrupted and resuspended in cold sterile double distilled water by rapidly scraping them from the plate surface using sterile micropipette tips and the suspensions were immedi-

ately incubated with an appropriate volume of RNA protect (Qiagen). The mixture was pelleted by centrifugation at 10,000g for 10 min and collected for RNA extraction using the RNeasy Mini Kit (Qiagen, Stockach, Germany) following the manufacturer's instructions. cDNA was prepared using M−MLV reverse transcriptase (Enzynomics, Korea) according to the manufacturer's instructions.

For gene quantitative real-time PCR, the PCR mixtures (20 μL) contained 1 μL of cDNA, primers (1 μM concentration, Table 1), and 10 μL TOPreal™ qPCR 2X PreMIX (SYBR Green with low ROX) master mix. The replication process involved denaturation step at 95 ℃ for 10 s, followed by 35 cycles of 95 ℃ for 15 s, 60 ℃ for 20 s, and 72 ℃ for 20 s. Each measurement was performed in three independent experiments. Data were analyzed using Bio-Rad CFX manager software and calculation of gene expression levels were normalized to the signal of the reference gene 16S rRNA.

2.8. Statistical analysis

Data are presented as the mean ± standard deviation (SD). The Student's t-test was used to calculate the significance of the difference between the mean expression of experimental and control samples. The level of significance was set at 5%.

3. Results

3.1. Biofilm formation and eradication

Strong biofilm production by SA is an important virulence factor of this organism. The effect of nanoAMG on biofilm formation by SA NCTC6571 and MRSA252 was measured in 96-well polystyrene plates. The test agents were added into the culture medium at the beginning of biofilm growth to analyse activity against biofilm formation (Fig. 1).

The results showed that at a concentration of 12 μmol/L, nanoAMG (black bars) showed an inhibition of biofilm biomass, up to about 42% and 25% for NCTC6571 and MRSA252 strains, respectively. This inhibition was less when the samples were treated with free AMG (white bars; about 24% and 10% inhibition, respectively). At the concentration of 24 μmol/L, nanoAMG still showed a stronger inhibitory activity by reducing biofilm biomass up to 62% and 53% for NCTC6571 and MRSA252 strains, respectively, while treatment with AMG resulted in inhibition of 44% and 39%, repectively. Treatment with 48 μmol/L nanoAMG resulted in disrupted biofilms up to > 80% for the both strains. To verify if the activity of nanoAMG was solely due to AMG, or whether the

carrier also influenced the results, the unloaded carrier was also tested. This, however, did not have any activity (data not shown).

When testing biofilm eradication, i.e. adding the compounds after 24 h of biofilm growth, AMG and nanoAMG were far less effective, and the biomass in the biofilms was reduced only by 27% and 22% when treated with nanoAMG at a concentration as high as 48 μmol/L for the NCTC6571 and MRSA 252, respectively (Fig. 2). This was, however, still better than free AMG, which did not have any activity against preformed biofilms.

3.2. Effects on bacterial adherence

Bacterial adherence is an initial step for biofilm formation. One of the strategies to control biofilm-related infections is to prevent both tissue colonization and biofilm formation by inhibiting bacterial adhesion. In this experiment, the effect of AMG and nanoAMG on the initial adherence of bacteria on polystyrene surface was investigated. The results in Fig. 3 show that both AMG and nanoAMG strongly inhibited bacterial adherence to polystyrene of both SA NCTC6571 and MRS252. AMG at a concentration of 12 μmol/L inhibited about 33% and 42% for MRSA252 and NCTC6571, respectively, while the nanoAMG inhibited up to 54% and 65%, respectively.
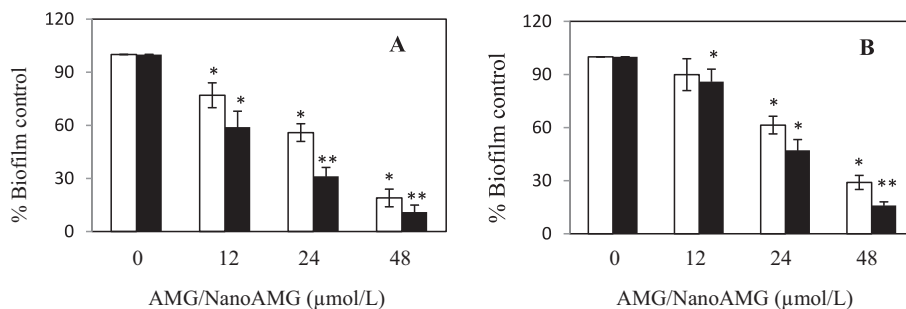
3.3. Cell death

To determine the efficacy of nanoAMG to kill *S. aureus* cells in biofilms, bacteria were grown for 48 h on polyvinyl coverslips (22 mm × 22 mm) in TSBg medium containing nanoAMG at a concentration of 48 μmol/L, with the medium being replaced with fresh nanoAMG-containing medium after 24 h. The biofilms were then analysed using two fluorescent nucleic acids staining agents, SYTO 9 and propidium iodide (PI). The treated biofilms clearly fluorescence red, which indicates that the bacteria are dead, whereas the fluorescence of the *S. aureus* biofilm was mainly green in the control samples without treatment (Fig. 4). This observation was similar to that of free AMG which was reported previously (Nguyen et al., 2017).

3.4. Gene expression

Recently, AMG was reported to suppress biofilm accumulation by SA strains (Nguyen et al., 2017). However, the effects of AMG/-nanoAMG on the expression of genes responsible for biofilm formation by SA have not been investigated, especially in SA strains with different biofilm structures (polysaccharide-based and protein-based biofilms). Therefore, in this study, we profiled the transcription of the selected genes involved in biofilm formation by SA under treatment with AMG or nanoAMG at 12 μmol/mL. Atshan et al. (2013) reported a number of genes that were found to be highly overexpressed during biofilm growth, which were *icaC*, *clfB*, *fnbA*, *fnbB* and *ebpS*. These genes were therefore selected to study the effects of AMG and nanoAMG. The data presented in Table 2 show the interesting result that *ebpS* was downregulated in MRSA252, but upregulated in NCTC6571, while the reverse was observed for *fnbB*. The genes *icaC*, *clfB* and *fnbA* were down regulated in both SA strains.

4. Discussion

>80% of human bacterial infections are reportedly biofilm associated (Song et al., 2018). It is clear that microbial biofilms are largely responsible for the resistance of many infections to conventional antimicrobial therapies. Natural compounds that exhibit antibiofilm activity have been documented previously.

Table 1
PCR primers sequences.

Gene	Functional category	Sequence primer (5′-3′)	Reference
fnbA	Fibronectin binding protein A	Fw: CAGTAGCTGAATTCCCATTTTCTTC Rv: AAATTGGGAGCAGCATCAGT	Atshan et al., (2013)
fnbB	Fibronectin binding protein B	Fw: ACGCTCAAGGCGACGGCAAAGRv: ACCTTCTGCATGACCTTCTGCACC	
ebps	Elastin binding protein	Fw: GCTGCGCCTCCAGCCAAACCT Rv: GTGCAGCTGGTGCAATGGGTGT	
icaC	Intercellular adhesion	Fw: TCTTGGGTATTTGCACGCAT Rv: GCAATATCATGCCGACACCT	Yu et al. (2012)
clfB	Clumping factor B	Fw: CTGGACTTGGTTCTGGATCTG Rv: ACGTTATGGTGGTGGAAGTG	
16 s rRNA	Reference gene	Fw: GGGACCCGCACAAGCGGTGG Rv: GGGTTGCGCTCGTTGCGGGA	This study

Fig. 1. NanoAMG inhibits biofilm formation by SA strains NCTC6571(A) and MRSA252 (B). AMG (□); nanoAMG (■). Biofilms were grown in TSBg media containing AMG and nanoAMG at different concentrations for 24 h at 37 °C. Biofilm biomass was assessed by staining with 0.1% crystal violet, which was then dissolved with 30% acetic acid followed by measuring the absorbance at λ = 595 nm (A_{595}). Data are expressed as the mean ± standard deviation. Data marked with * are significantly different with $p < 0.05$ and ** with $p < 0.01$.
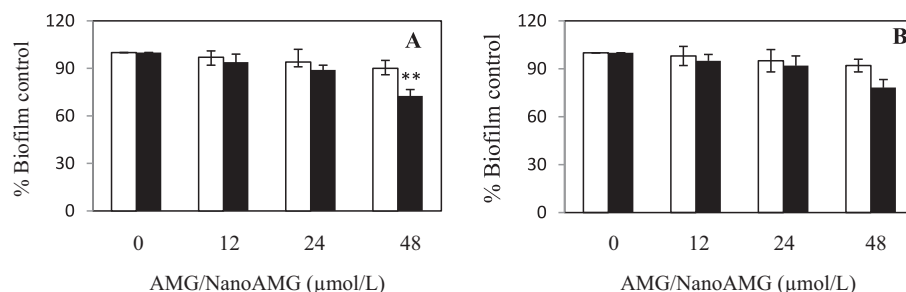
Fig. 2. NanoAMG inhibits preformed biofilm by SA strains NCTC6571(A) and MRSA252 (B). AMG (□); nanoAMG (■). Biofilms were grown in TSBg media containing AMG and nanoAMG at different concentrations for 24 h at 37 °C. Biofilm biomass was assessed by staining with 0.1% crystal violet, which was dissolved with with 30% acetic acid and followed by measuring the absorbance at λ = 595 nm (A_{595}). Data are expressed as the mean ± standard deviation. Data marked with * are significantly different with $p < 0.05$ and ** with $p < 0.01$.
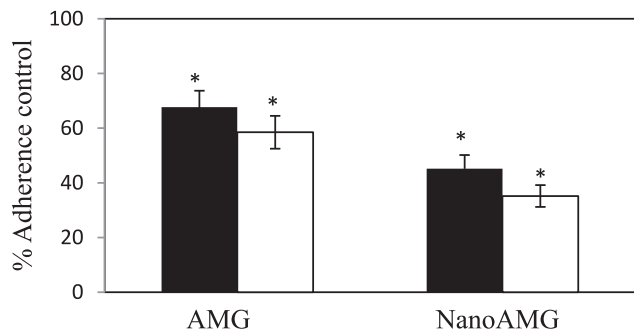

Fig. 3. Effect of nanoAMG on initial adherence of *S. aureus* NCTC6571 (□) and MRSA252 (■). Bacteria were grown in TSBg media containing AMG and nanoAMG at different concentration of 12 μmol/L for 4 h at 37 °C. The adhered bacteria were assessed by staining with 0.1% crystal violet solution, which was dissolved with 30% acetic acid and followed by measuring the absorbance at λ = 595 nm (A_{595}). Data are expressed as the mean ± standard deviation. Data marked with * are significantly different with $p < 0.05$.

For example, myricetin and proanthocyanidin from cranberry decreased the production of insoluble extracellular polymeric substance (EPS) by 80% in *S. mutans* (Kim et al., 2015). Furthermore, rhodomyrtone from the leaves of *Rhodomyrtus tomentosa* (Aiton) Hassk at a concentration of approximately 100 μM could inhibit biofilm formation by *S. epidermidis* ATCC 35,984 and *S. pneumonia* (Saising et al., 2011). Eugenol from *Syzygium aromaticum* and *Cinnamomum zeylanicum* could inhibit biofilm inhibition by *S. aureus* on polystyrene and stainless steel (52.8 and 19.6%, respectively) at a concentration of 0.1 mg/ml (Song et al., 2018).

AMG, a valuable bioactive xanthone compound that is enriched in the pericarps of the tropical fruit mangosteen, has been reported to possess anti-biofilm activity against *S. mutans* and *S. aureus*, including MRSA strains, through the distruption of biofilm formation at concentrations of 100 μM (Nguyen et al., 2014, 2017). However, the potential use of AMG on preventing the biofilm formation is problematic due to its low solubility, leading to a low bioavailability. In this study, to overcome this limitation, polymeric nanoparticles of AMG were synthesized and these were, for the first time, tested for antibiofilm activity on two SA strains including the reference strain NCTC6571 and the multiresistant strain MRSA252. These strains were chosen as they have different biofilm structures, forming polysaccharide and protein-based biofilms, respectively.

Nanoparticle preparation enhances the microbial activity of many compounds, as shown for instance for nanoberberin (Sahibzada et al., 2018). AMG coated nanoparticles for different therapeutic purposes have also been studied. Pan-In et al. (2014, 2015) have successfully synthesized nanoAMG to treat *Propionibacterium acnes* and *Helicobacter pylori*. Yao et al. (2016) have prepared nanoAMG using polyethylene glycol-polylactic acid as a delivery system to treat Alzheimer's disease. The nanoparticles improved distribution in organs such as the brain and liver. Ramadhan and Krisanti (2018) reported a AMG nanoemulsion that penetrated the skin layer up to 12 μg/cm^2. For treatment of oral diseases, Zhou et al. (2016) and Ren et al. (2019) reported the use of cationic, pH-responsive p(DMAEMA)-*b*-p(DMAEMA-co-BMA-co-PAA) block copolymer micelles of the natural compound farnesol with high affinity for dental and biofilm surfaces and efficient anti-bacterial drug release in response to acidic pH, characteristic of cariogenic (tooth-decay causing) biofilm microenvironments. So far, the synthesis of nanoAMG for the treatment of biofilms related to diseases had not been implemented. By using a modified method for the preparation of polymeric
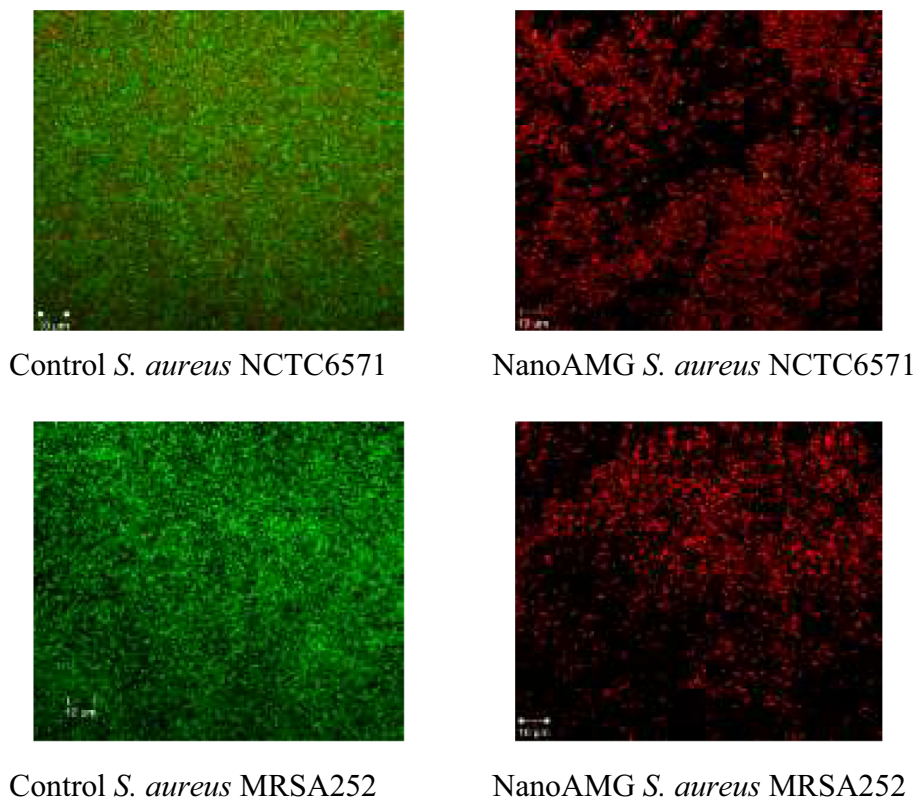
Fig. 4. Confocal microscopy images of *S. aureus* NCTC6571 and MRSA 252 biofilms grown on coverslips with nanoAMG. Biofilms of *S. aureus* were cultured for 48 h at 37 °C in fresh TSBg medium (Control) or in TBSg medium supplemented with 48 µmol/L NanoAMG. The coverslips were then stained for 15 min with LIVE/DEAD BacLight mixture (50:50 v/v). Stained biofilms were observed using laser scanning confocal fluorescence microscopy. The dead cells are red, while living cells show up as green.

Table 2
Fold change (log$_2$ transformed) in mRNA levels of target genes *fnbA, fnbB, icaC, ebpS* and *clfB* in biofilms of *S. aureus* NCTC6571 and MRSA252 after treatment with AMG and nanoAMG.

Log$_2$ Fold change in level of biofilm genes				
Gene	NCTC6571		MRSA252	
	AMG	NanoAMG	AMG	NanoAMG
16 s rRNA[a]	0.00	0.00	0.00	0.00
fnbA	−4.64[(*)]	−1.69	−1.12	−5.64
fnbB	−3.64	−5.06	2.91	4.25
ebpS	3.00	1.72	−2.47	−5.06
icaC	−3.06	−3.64	−0.76	−1.40[(*)]
clfB	−4.64	−0.27	−0.84	0.06[(*)]

[a] 16s rRNA was used as reference gene for the experiments. All values showed a significant change in expression as compared to the untreated control ($P < 0.05$), except for the values indicated with a * ($P > 0.05$).

nanoparticle of AMG, we successfully synthesized nanoAMG particles with sizes in the range of 10–50 nm and enhanced solubility compared to free AMG (of which solubility in water is only 0.2 µg/mL) (Aisha et al., 2012). The data indicated that the particles exhibited a clearly improved inhibitory activity against biofilm production by SA strains as compared to the unloaded AMG, especially in the early stages of biofilm formation. On preformed (24 h) biofilms, however, the bacteria were more recalcitrant to AMG and nanoAMG, which may be caused by their limited diffusion into the biofilms of SA strains. Nevertheless, nanoAMG showed an enhanced antibiofilm activity as compared to free AMG on both biofilm formation and biofilm eradication, indicating that AMG availability was improved by using a nanoparticle formulation.

In our previous study we found that the two SA strains had different sensitivity to AMG in which MRSA252 is more resistant to AMG than NCTC6571. The biofilm structures of two these strains are different, as MRSA252 produces EPS mainly containing protein,

whereas the EPS of NCTC6571 mainly contains polysaccharides (Nguyen et al., 2017). The difference in biofilm structure may relate to the AMG sensitivity of two these strains and we hypothesized that the proteinaceous biofilm matrix of MRSA252 provides better protection by binding AMG. To this purpose we analysed the expression of several biofilm-related genes in the two strains that were treated with AMG or nanoAMG. There were some interesting differences when comparing the two strains with each other. Firstly, the expression of *icaC* was suppressed to a much greater extent in NCTC6571 as compared to MRSA252. This gene encodes a transporter that is involved in the production of the biofilm adhesin poly-beta-1,6-N-acetyl-D-glucosamine (PNAG) (Atkin et al., 2014). PNAG is also likely to be the main constituent of the polysaccharide-based matrix of NCTC6571, while, as mentioned before, the extracellular matrix of MRSA252 mainly contains protein. Thus, it seems likely that AMG or nanoAMG has a greater effect on the EPS of NCTC6571 as compared to MRSA252. This

could explain the increased sensitivity to AMG or nanoAMG of the former strain, which supports our hypothesis that sensitivity to AMG/nanoAMG is be related to the composition of the EPS. Another curious observation was that after treatment with AMG or nanoAMG, *fnbB* expression was clearly down-regulated in NCTC6571 but this gene was up-regulated in MRSA252. The gene product of *fnbB* appears to be responsible for increased levels of resistance observed in highly resistant subpopulations of heterogeneous MRSA, suggesting *fnbB* may play a role in the response to environmental conditions (Aedo and Tomasz, 2016). In contrast, the expression of *ebpS* was suppressed in MRSA252 but enhanced in NCTC6571. It is known that the gene product of *ebpS* is involved in binding of SA to the host protein elastin, thereby facilitating attachment, colonization, and invasion of the bacteria. Moreover, *ebpS* also plays a role in the regulation of growth of *S. aureus* (Downer et al., 2002). However, it is at this stage not clear what these results with *fnbB* and *ebpS* expression mean in relation to the response to AMG or nanoAMG, and further research is required to explain these observations. The other genes tested relating to bacterial adhesion included *clfB* and *fnbA* (Lim et al., 2015), which were down-regulated in both SA strains after treatment with AMG or nanoAMG. Taken together, our data provide new findings indicating a relationship between AMG resistance and biofilm structure, and we show a number of genes that are involved in this.

We also speculated that, because nanoAMG appears more effective than AMG, that this might be reflected in differences in gene expression in the biofilm-related genes. However, while absolute levels of gene expression did vary to some degree when comparing the two drug formulations, there was no clear pattern in this, which is probably a reflection of the complex multifactorial process of biofilm formation. We should also point out that the differences in sensitivity to AMG or nanoAMG between the strains is fairly subtle, and of course other genes are also involved in the regulation of biofilm formation. For instance, McCarthy et al, (2015) indicated that the release of cell surface expression of a number of sortase-anchored proteins and the major autolysin have been implicated in the biofilm phenotype of MRSA isolates. Obviously, more investigations on the genes involved in biofilm pathways are necessary to fully understand the actions of AMG and nanoAMG on biofilm synthesis by SA strains for practical application.

5. Conclusions

Our findings suggest that incorporation of AMG into polymer nanoparticles potentially results in better efficacy for biofilm treatment, especially at early phases of biofilm formation by SA, including MRSA. It seems to have a relationship between AMG resistance and biofilm structure as well as, there are genes that are involved in this. Nevertheless, for fully understand of action mechanisms and therapeutic application, further work on the antibiofilm activity of nanoAMG, for instance, mixed biofilm models, and *in vivo* studies regarding toxicity, pharmacokinetic profile and bioavailability are still needed.

Authors' contributions

NTMP designed the project, supervised and performed the experiments, analyzed data and wrote the manuscript. AB revised the research and the manuscript. NTHM performed the experiments, and analyzed data. All authors have read and approved the final manuscript.

Declaration of Competing Interest

The authors declare that they have no competing interests.

Acknowledgments

Appendix A. Supplementary material

Supplementary data to this article can be found online at https://doi.org/10.1016/j.sjbs.2020.11.061.

References

Aedo, S., Tomasz, A., 2016. Role of the stringent stress response in the antibiotic resistance phenotype of methicillin-resistant *Staphylococcus aureus*. Antimicrob. Agents Chemother. 60 (4), 2311–2317. https://doi.org/10.1128/AAC.02697-15.

Aisha, A.F., Ismail, Z., Abu-Salah, K.M., Majid, A.M., 2012. Solid dispersions of α-mangostin improve its aqueous solubility through self-assembly of nanomicelles. J. Pharm. Sci. 101 (2), 815–825. https://doi.org/10.1002/jps.22806.

Alhusein, N., De Bank, P.A., Blagbrough, I.S., Bolhuis, A., 2013. Killing bacteria within biofilms by sustained release of tetracycline from triple-layered electrospun micro/nanofibre matrices of polycaprolactone and poly(ethylene-co-vinyl acetate). Drug Deliv. Transl. Res. 3 (6), 531–541. https://doi.org/10.1007/s13346-013-0164-9.

Archer, N.K., Mazaitis, M.J., Costerton, J.W., Leid, J.G., Powers, M.E., Shirtliff, M.E., 2011. Staphylococcus aureus biofilms: Properties, regulation, and roles in human disease. Virulence. 2 (5), 445–459. DOI: 10.4161/viru.2.5.17724.

Atkin, K.E., MacDonald, S.J., Brentnall, A.S., Potts, J.R., Thomas, G.H., 2014. A different path: Revealing the function of staphylococcal proteins in biofilm formation. FEBS Lett. 588 (10), 1869–1872. https://doi.org/10.1016/j.febslet.2014.04.002.

Atshan, S.S., Shamsudin, M.N., Karunanidhi, A., van Belkum, A., Lung, L.T., Sekawi, Z., Nathan, J.J., Ling, K.H., Seng, J.S., Ali, A.M., Abduljaleel, S.A., Hamat, R.A., 2013. Quantitative PCR analysis of genes expressed during biofilm development of methicillin resistant *Staphylococcus aureus* (MRSA). Infect. Genet. Evol. 18, 106–112. https://doi.org/10.1016/j.meegid.2013.05.002.

Burke, F.M., McCormack, N., Rindi, S., Speziale, P., Foster, T.J., 2010. Fibronectin-binding protein B variation in *Staphylococcus aureus*. BMC Microbiol. 10, 160. https://doi.org/10.1186/1471-2180-10-160.

Dastgheyb, S., Parvizi, J., Shapiro, I.M., Hickok, N.J., Otto, M., 2014. Effect of biofilms on recalcitrance of Staphylococcal joint infection to antibiotic treatment. J. Infect. Dis. 211, 641–650. https://doi.org/10.1093/infdis/jiu514.

Downer, R., Roche, F., Park, P.W., Mecham, R.P., Foster, T.J., 2002. The elastin-binding protein of *Staphylococcus aureus* (EbpS) is expressed at the cell surface as an integral membrane protein and not as a cell wall-associated protein. J. Biol. Chem. 277 (1). https://doi.org/10.1074/jbc.M107621200.

Fey, P.D., 2010. Olson ME. Current concepts in biofilm formation of *Staphylococcus epidermidis*. Future Microbiol. 5 (6), 917–933. https://doi.org/10.2217/fmb.10.56.

Flemming, H.C., Wingender, J., 2009. The biofilm matrix. Nat. Rev. Microbiol. 8, 623–633. https://doi.org/10.1038/nrmicro2415.

Foulston, L., Elsholz, A.K., DeFrancesco, A.S., Losick, R., 2014. The extracellular matrix of *Staphylococcus aureus* biofilms comprises cytoplasmic proteins that associate with the cell surface in response to decreasing pH. MBio. 5 (5), e01667–e01714. https://doi.org/10.1128/mBio.01667-14.

Greenberg, M., Dodds, M., Tian, M., 2008. Naturally occurring phenolic antibacterial compounds show effectiveness against oral bacteria by a quantitative structure–activity relationship study. J. Agric. Food Chem. 56 (23), 11151–11156. https://doi.org/10.1021/jf8020859.

Gunasekaran, T., Haile, T., Nigusse, T., Dhanaraju, M.D., 2014. Nanotechnology: an effective tool for enhancing bioavailability and bioactivity of phytomedicine. APJTB. 4 (Suppl 1), S1–S7. https://doi.org/10.12980/APJTB.4.2014C980.

Hall-Stoodley, L., Stoodley, P., 2009. Evolving concepts in biofilm infections. Cell Microbiol. 11 (7), 1034–1043. https://doi.org/10.1111/j.1462-5822.2009.01323.x.

Holden, M.T., Feil, E.J., Lindsay, J.A., Peacock, S.J., Day, N.P., Enright, M.C., et al., 2004. Complete genomes of two clinical *Staphylococcus aureus* strains: Evidence for the rapid evolution of virulence and drug resistance. PNAS USA 101, 9786–9791. https://doi.org/10.1073/pnas.0402521101.

Ibrahim, M.Y., Hashim, N.M., Mariod, A.A., Mohan, S., Abdulla, M.A., Abdelwahab, S. I., Arbab, I.A., 2016. α-Mangostin from *Garcinia mangostana* Linn: An updated review of its pharmacological properties. Arab. J. Chem. 9 (3), 317–329. https://doi.org/10.1016/j.arabjc.2014.02.011.

Kim, D., Hwang, G., Liu, Y., Wang, Y., Singh, A.P., Vorsa, N., Koo, H., 2015. Cranberry flavonoids modulate cariogenic properties of mixed-species biofilm through exopolysaccharides-matrix disruption. PLoS One. 10, (12). https://doi.org/10.1371/journal.pone.0145844 e0145844.

Kong, C., Chin-Fei, C., Richter, K., Thomas, N., Rahman, A., Nathan, S., 2018. Suppression of *Staphylococcus aureus* biofilm formation and virulence by a

benzimidazole derivative, UM-C162. Sci. Rep. 8, 2758. https://doi.org/10.1038/s41598-018-21141-2.

Koo, H., Allan, R.N., Howlin, R.P., Stoodley, P., Hall-Stoodley, L., 2017. Targeting microbial biofilms: current and prospective therapeutic strategies. Nat. Rev. Microbiol. 15 (12), 740–755. https://doi.org/10.1038/nrmicro2017.99.

Lim, S., Lee, D.H., Kwak, W., Shin, H., Ku, H.J., Lee, J.E., Lee, G.E., Kim, H., Choi, S.H., Ryu, S., Lee, J.H., 2015. Comparative genomic analysis of Staphylococcus aureus FORC_001 and S. aureus MRSA252 reveals the characteristics of antibiotic resistance and virulence factors for human infection. J. Microbiol. Biotechnol. 25 (1), 98–108. https://doi.org/10.4014/jmb.1410.10005.

McCarthy, H., Rudkin, J.K., Blac, N.S., Gallagher, L., O'Neill, E., O'Gara, J.P., 2015. Methicillin resistance and the biofilm phenotype in Staphylococcus aureus. Front. Cell. Infect. Microbiol. 5, 1–9. https://doi.org/10.3389/fcimb.2015.00001.

Nguyen, P.T.M., Falsetta, M.L., Hwang, G., Gonzale, M., Koo, H., 2014. α-Mangostin disrupts the development of Streptococcus mutans biofilms and facilitates its mechanical removal. PloS One. 9, (10). https://doi.org/10.1371/journal.pone.0111312 e1113122014.

Nguyen, P.T.M., Ngo, V.Q., Ta, T.M., Nguyen, V.A., Kuhakarn, C., Reutrakul, V., Bolhuis, A., 2017. Antibiofilm activity of α-mangostin extracted from Garcinia mangostana L. against Staphylococcus aureus. APJTM. 10 (12), 1154–1160. https://doi.org/10.1016/j.apjtm.2017.10.022.

Nguyen, H.M., Nguyen, T.D., Nguyen, T.M.P., 2020. Apoptosis induction by α-mangostin-loaded nanoparti, cles against human cervical carcinoma cells. ZNC. 75 (5–6), 145–151. https://doi.org/10.1515/znc-2020-0001.

O'Neill, E., Pozzi, C., Houston, P., Humphreys, H., Robinson, D.A., Loughman, A., Foster, T.J., O'gara, J.P., 2008. A novel Staphylococcus aureus biofilm phenotype mediated by the fibronectin-binding proteins, FnBPA and FnBPB. J. Bacteriol. 190, 3835–3850. https://doi.org/10.1128/JB.00167-08.

Oniciuc, E., NunoCerca, N., Nicolau, A., 2016. Compositional analysis of biofilms formed by Staphylococcus aureus isolated from food sources. Front. Microbiol. fmic.00390. https://doi.org/10.3389/fmicb.2016.00390.

Pan-In, P., Tachapruetinun, A., Chaichanawongsaroj, N., Banlunara, W., Suksamrarn, S., Wanichwecharungruang, S., 2014. Combating Helicobacter pylori infections with mucoadhesive nanoparticles loaded with Garcinia mangostana extract. Nanomedicine (Lond) 9 (3), 457–468. https://doi.org/10.2217/nnm.13.30.

Pan-In, P., Wongsomboon, A., Kokpol, C., Chaichanawongsaroj, N., Wanichwecharungruang, S., 2015. Depositing α-mangostin nanoparticles to sebaceous gland area for acne treatment. J. Pharmacol. Sci. 129 (4), 226–232. https://doi.org/10.1016/j.jphs.2015.11.005.

Phitaktim, S., Chomnawang, M., Sirichaiwetchakoon, K., Dunkhunthod, B., Hobbs, G., Eumkeb, G., 2016. Synergism and mechanism of action of α-mangostin isolated from Garcinia mangostana L. and oxacillin combination against oxacillin-resistant Staphylococcus saprophyticus. BMC Microbiol. 16 (1), 195. https://doi.org/10.1186/s12866-016-0814-4.

Rabin, N., Zheng, Y., Opoku-Temeng, C., Du, Y., Bonsu, E., Sintim, H.O., 2015. Biofilm formation mechanisms and targets for developing antibiofilm agents. Future Med. Chem. 7 (4), 493–512. https://doi.org/10.4155/fmc.15.6.

Ramadhan, M.K., Krisanti, E.A., 2018. Formulation and characterization of nanoemulsion gel mangosteen extract in virgin coconut oil for topical formulation. MATEC Web Conf. 156, 1–7. https://doi.org/10.1051/matecconf/201815601013.

Ren, Z., Kim, D., Paula, A.J., Hwang, G., Liu, Y., Li, J., Daniell, H., Koo, H., 2019. Dual-targeting approach degrades biofilm matrix and enhances bacterial killing. J. Dent. Res. 98 (3), 322–330. https://doi.org/10.1177/0022034518818480.

Rodrigues, L.R., Banat, M.I., van Der Mei, H.C., Teixeira, J.A., Oliveira, R., 2006. Interference in adhesion of bacteria and yeasts isolated from explanted voice prostheses to silicone rubber by rhamnolipid biosurfactants. J. Appl. Microbiol. 100, 470–480. https://doi.org/10.1111/j.1365-2672.2005.02826.x.

Sahibzada, M.U.K., Sadiq, A., Faidah, H.S., Khurram, M., Amin, M.U., Haseeb, A., Kakar, M., 2018. Berberine nanoparticles with enhanced in vitro bioavailability: characterization and antimicrobial activity. Drug Des. Dev. Ther. 12, 303–312. https://doi.org/10.2147/DDDT.S156123.

Saising, J., Ongsakul, M., Voravuthikunchai, S.P., 2011. Rhodomyrtus Tomentosa (Aiton) Hassk. Ethanol extract and rhodomyrtone: A potential strategy for the treatment of biofilm-forming Staphylococci. J. Med. Microbiol. 60 (Pt 12), 1793–1800. https://doi.org/10.1099/jmm.0.033092-0.

Shivaee, A., Kalani, B.S., Talebi, M., Darban-Sarokhalil, D., 2019. Does biofilm formation have different pathways in Staphylococcus aureus?. Iran. J. Basic Med. Sci. 2 (10), 1147–1152. https://doi.org/10.22038/ijbms.2019.34888.8281.

Sivaranjani, M., Prakash, M., Gowrishankar, S., Rathna, J., Pandian, S.K., Rav, A.V., 2017. In vitro activity of alpha-mangostin in killing and eradicating Staphylococcus epidermidis RP62A biofilms. Appl. Microbiol. Biotechnol. 101 (8), 3349–3359. https://doi.org/10.1007/s00253-017-8231-7.

Sivaranjani, M., Srinivasan, R., Aravindraja, C., Karutha, P.S., Veera-Ravi, A.R., 2018. Inhibitory effect of α-mangostin on Acinetobacter baumannii biofilms - an in vitro study. Biofouling. 234 (5), 579–593. https://doi.org/10.1080/08927014.2018.1473387.

Song, X., Xia, Y.X., Zhen-Dan, H., Zhang, H., 2018. A review of natural products with anti-biofilm activity. Curr. Org. Chem. 22, 788–816. https://doi.org/10.1186/s13020-019-0232-2.

Speziale, P., Pietrocola, G., Foste, T.J., Geoghegan, J.A., 2014. Protein-based biofilm matrices in Staphylococci. Front. Cell. Infect. Microbiol. 10 (4), 171. https://doi.org/10.3389/fcimb.2014.00171.

Vergara-Irigaray, M., Valle, J., Merino, N., Latasa, C., García, B., de Los, R., Mozos, I., Solano, C., Toledo-Arana, A., Penadés, J.R., Lasa, I., 2009. Relevant role of fibronectin-binding proteins in Staphylococcus aureus biofilm-associated foreign-body infections. Infect. Immun. 77 (9), 3978–3991. https://doi.org/10.1128/IAI.00616-09.

Wang, M., Zhang, K., Gu, Q., Bi, X., Wang, J., 2017. Pharmacology of mangostins and their derivatives: A comprehensive review. Chin. J. Nat. Med. 15 (2), 81–93. https://doi.org/10.1016/S1875-5364(17)30024-9.

Yao, L., Gu, X., Song, Q., Wang, X., Huang, M., Hu, M., Hou, L., Kang, T., Chen, J., Chen, H., Gao, X., 2016. Nanoformulated alpha-mangostin ameliorates Alzheimer's disease neuropathology by elevating LDLR expression and accelerating amyloid-beta clearance. J. Control. Release 226, 1–14. https://doi.org/10.1016/j.jconrel.2016.01.055.

Yu, D., Zhao, L., Xue, T., Sun, B., 2012. Staphylococcus aureus autoinducer-2 quorumsensing decreases biofilm formation in anicaR-dependent manner. BMC Microbiol. 12, 288. https://doi.org/10.1186/1471-2180-12-288.

Zhou, J., Horev, B., Hwang, G., Klein, M.I., Koo, H., Benoit, D.S., 2016. Characterization and optimization of pH-responsive polymer nanoparticles for drug delivery to oral biofilms. J. Mat. Chem. b. 4 (18), 3075–3085. https://doi.org/10.1039/C5TB02054A.